

Mariner 6 and 7 Ultraviolet Spectrometers

J. B. Pearce, K. A. Gause, E. F. Mackey, K. K. Kelly, W. G. Fastie, and C. A. Barth

The ultraviolet spectrometers that observed the atmosphere of Mars in July and August of 1969 consist of a planetary coronagraph and an Ebert-Fastie monochromator. The spectral range 1100–4300 Å was measured using two photomultiplier tubes, one with a cesium iodide photocathode, the other with a bialkali photocathode. These tubes were operated with fixed high voltage supplies and charge sensitive amplifiers. The instruments were calibrated by comparison with a tungsten lamp, a sodium salicylate screen, and a flowing nitric oxide cell. The instruments were able to satisfactorily reject off-axis light at a distance of 6600 km and measure the emission spectrum of the upper atmosphere 170 km above the surface.

Introduction

The Mariner 6 and 7 spacecraft approached and flew by Mars on 31 July 1969 and 5 August 1969, respectively. Each spacecraft carried a complement of scientific instruments that included a scanning ultraviolet spectrometer. The primary purpose of the ultraviolet spectrometer experiment was to determine the composition and structure of the atmosphere of Mars by measuring the ultraviolet light emitted by the upper atmosphere and the sunlight scattered by the lower atmosphere and surface.¹ Results on the Mars upper atmosphere experiment have been reported by Barth *et al.*² This paper describes the design and calibration of the spectrometer and demonstrates its performance at Mars.

Experiment Constraints

Two basic kinds of measurements were performed that can be most easily characterized by the observation geometries. The first, upper atmospheric measurements, were obtained viewing the atmosphere tangentially against the dark space background. The second, measurements of the surface pressure and reflectance, were made while viewing the planetary disk directly.

In order to detect radiations characteristic of a wide range of possible atmospheric constituents, the spectral

region 1100–4300 Å was scanned. Since the spacecraft moved at ~ 7 km sec⁻¹ relative to Mars, a spectral scan was made each 3 sec so that at least one measurement would be obtained every 21 km, the nominal atmospheric scale height. A study of the expected atmospheric features showed that a spectral resolution of 20 Å was sufficient to identify them, but a sensitivity of 100 R was required (a rayleigh is equal to 10^6 photons cm⁻² sec⁻¹). The ability of the instrument to reject off-axis light from the very bright planetary disk during the upper atmospheric measurements was critical to this part of the experiment. A high dynamic range was required to accommodate these weak signals and also the intense (10^4 R) signals expected during the surface pressure and reflectance measurements. To satisfy these constraints an Ebert-Fastie scanning monochromator with dual photomultiplier detectors was used in the focal plane of a reflecting planetary coronagraph.

Planetary Coronagraph

The coronagraph, described by Fastie,³ uses a 0.25-m focal length spherical primary mirror that forms an off-axis image of the atmosphere in an occulting slit plane (see Fig. 1). This mirror is aluminized and overcoated with MgF₂ in order to provide high reflectivity throughout the spectral range, as are all the optical surfaces in the instrument. In front of the mirror is a multiple baffle system (see Fig. 2) designed to prevent light from the planet's surface from striking the primary directly. A baffled secondary mirror transfers the atmospheric image, passed by the occulting slit, to the entrance slit of the monochromator. Also in the plane of the occulting slit are two near infrared sensitive photodiodes used as planetary limb sensors to control the dynamic range of the detector system. Figure 3 shows the image, formed by the coronagraph, of the monochromator entrance slit and the limb sensors in a

J. B. Pearce, K. A. Gause, K. K. Kelly, and C. A. Barth are with the Laboratory for Atmospheric and Space Physics, University of Colorado, Boulder, Colorado 80302; E. F. Mackey is with SpaCom Electronics, Camarillo, California 93010; W. G. Fastie is with the Physics Department, Johns Hopkins University, Baltimore, Maryland 21218.

Received 12 October 1970.

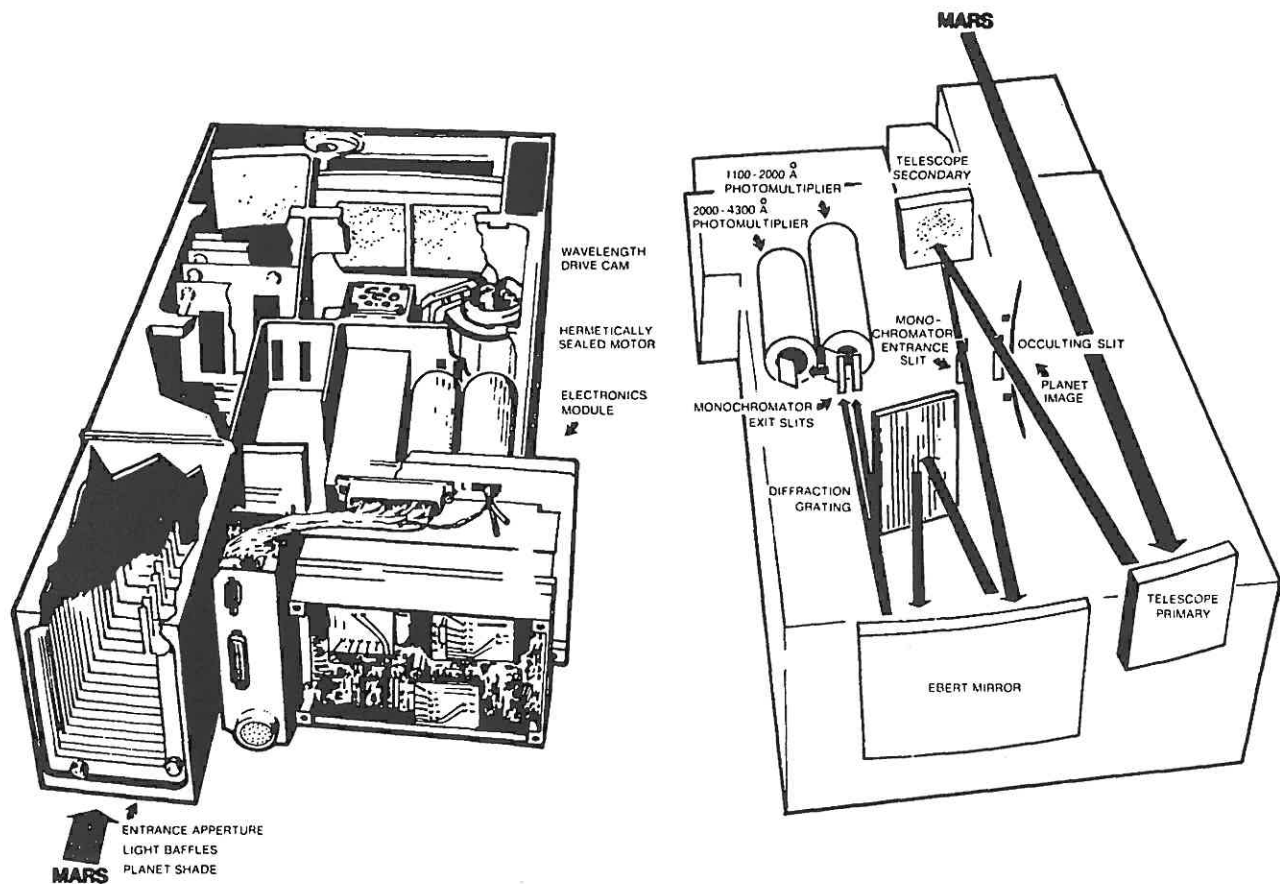


Fig. 1.
A ghost view of the Mariner 6 and 7 ultraviolet spectrometer showing the location of various parts and a schematic ray path.

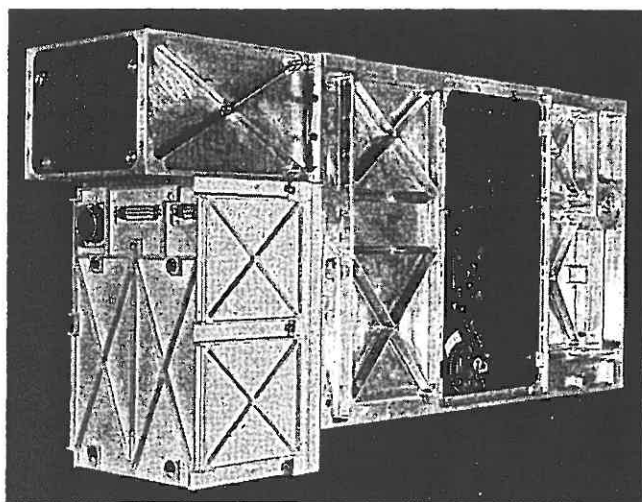


Fig. 2. The Mariner 6 and 7 ultraviolet spectrometer. The detector and electronics assembly is at the bottom in the foreground with connectors. Above is the viewing port with the coronagraph baffles showing. Visible in the main housing are additional baffles above and the wavelength drive cam in the monochromator below.

plane perpendicular to the optical axis and containing the planet's center.

Ebert-Fastie Monochromator

The Ebert⁴-Fastie⁵⁻⁷ monochromator uses a plane diffraction grating and a single spherical mirror. The monochromator forms a spectrum of images of the entrance slit in the exit slit plane (see Fig. 4) for each diffraction order. A separate exit slit was provided for each of the two detectors. In operation, the position of the spectral images with respect to the exit slits is controlled by cyclically scanning the grating.

The grating is a 2160-lines mm^{-1} replica, blazed at 3000 Å. The first order is scanned so that the spectral range from 1900 Å to 4300 Å is covered in first order as seen by one of the two exit slits, and the range from 1100 Å to 2100 Å in second order by the other. The efficiency of a typical grating is shown in Fig. 5. A scan is made from low to high wavelengths in 2.82 sec and rapidly returned to low in 0.18 sec. The 56-mm by 64-mm ruled area of the diffraction grating subtends the limiting aperture of $f/4.2$. The spectral resolution of the instrument, which is a slowly varying function of

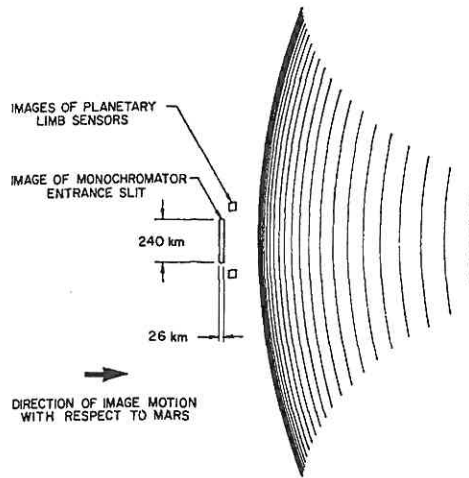


Fig. 3. The Mars atmospheric observation geometry just prior to a limb crossing.

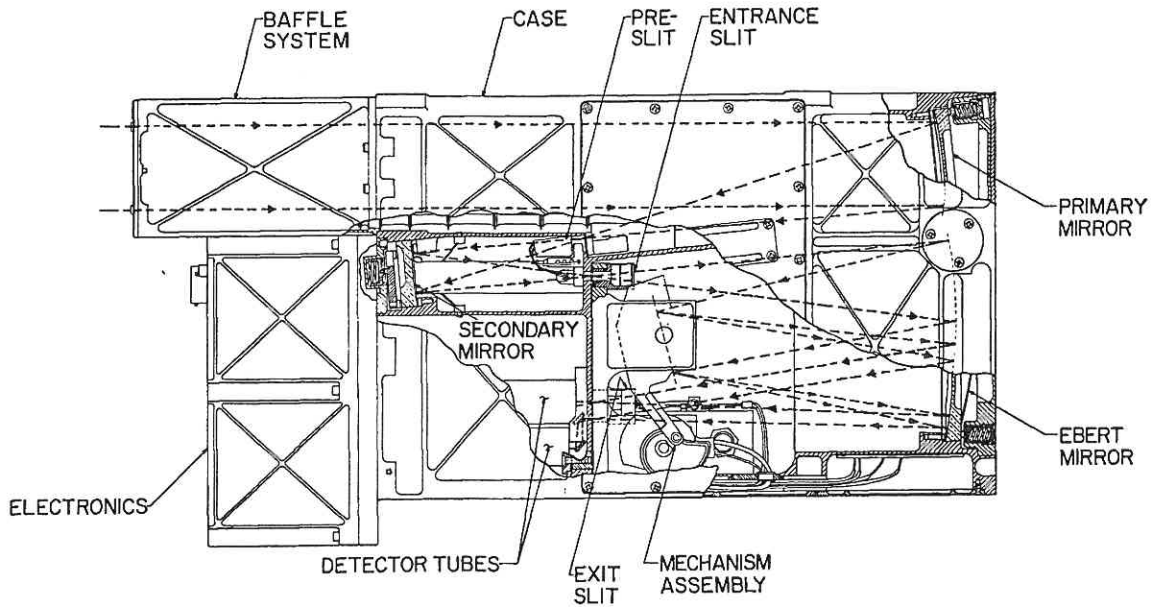


Fig. 4. A plan view drawing of the instrument with the extreme rays shown.

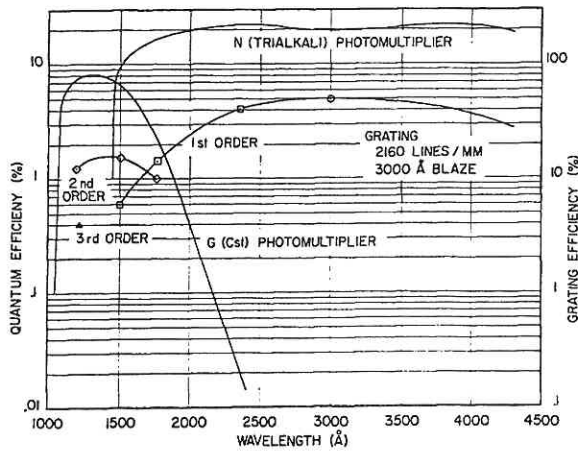


Fig. 5. Relative efficiency of gratings and photomultiplier tubes of the types used in the Mariner 6 and 7 ultraviolet spectrometers vs wavelength. Measurements were performed under simulated instrument conditions (symbols) and used for normalization of manufacturers specifications (lines).

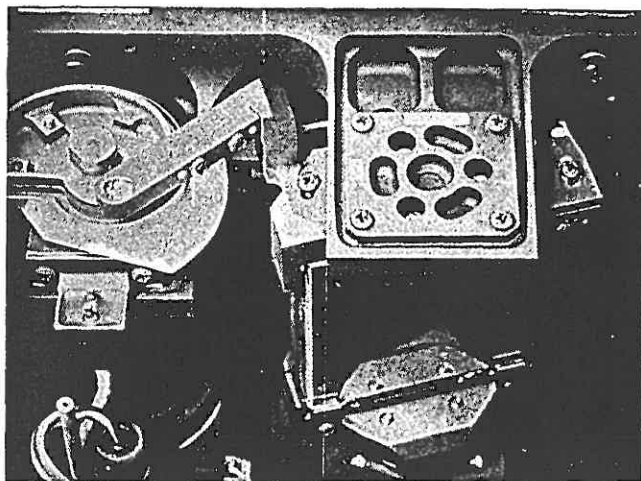


Fig. 6. Scan mechanism assembly showing grating, cam, and follower and the magnetic sensor for the fiducial marker. The motor and planocentric drive are beneath the cam.

wavelength, is 20 \AA at 2950 \AA in the first order as limited by the slit width.

The grating is rotated through about 16° during each spectral scan. The motion is controlled by a cam and follower driven by a two-phase hysteresis synchronous size 11 motor (see Fig. 6). The motor is driven by 300-cycle square wave power derived by counting down the 2400-Hz spacecraft power. This results in a pinion speed of 9000 rpm which is geared down to drive the cam at 20 rpm. To ensure proper lubrication and at the same time eliminate danger to the optics, the motor and gear train are hermetically sealed. The cam is driven by the ring gear of a planocentric gear set. The pinion of the planocentric pair is sealed to the motor housing with a bellows (see Fig. 7). The planocentric gear teeth that must run in hard vacuum are Nitroloy 135 M. All bearings running in hard vacuum are non-lubricated Bar Temp bearings.

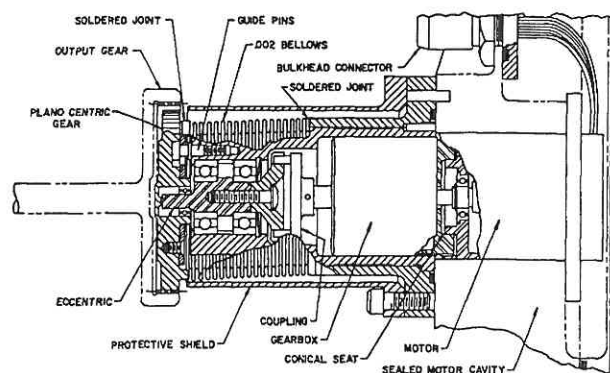


Fig. 7. Planocentric drive assembly showing the synchronous motor, gear box, and eccentric that drives the planocentric pinion. The cam is attached to the shaft of the output gear.

Detectors and Electronics

Two photomultiplier tubes are used as detectors. The one sensitive to light in the $1900\text{--}4300 \text{ \AA}$ spectral region is offset from its exit slit by a reflecting periscope; and the other, for second order light in the range from 1100 \AA to 2100 \AA , is mounted directly behind its exit slit (see Fig. 4). The photomultiplier tubes used are of the end window, semitransparent, high work function photocathode variety manufactured by EMR. They have an in-line venetian blind dynode structure and are, in this case, operated with the anode near ground potential. The longer wavelength sensitive tube used in the $1900\text{--}4300 \text{ \AA}$ range, the N channel, is a model 541N-05M which has a bialkali photocathode and a sapphire window. The other tube, sensitive from 1100 \AA to 2100 \AA , the G channel, is a model 541G-08 using a cleaved lithium fluoride window with a cesium iodide photocathode. The spectrum of light scattered from the surface and lower atmosphere is approximately that of the sun, an $\sim 5000 \text{ K}$ blackbody. In order to measure light in the $1100\text{--}1800 \text{ \AA}$ region it is necessary that the detector be insensitive to light at wavelengths longer than $\sim 2100 \text{ \AA}$ since the diffraction grating diffusely scatters a small fraction of this enormously brighter source. This rejection characteristic is a consequence of the high work function of the cesium iodide photocathode. The relative sensitivity of these photomultiplier tubes is shown in Fig. 5.

Figure 8 is a block diagram showing the operation of the electronics system. High voltage for the operation of the photomultipliers is supplied by independent ac to dc converter multipliers powered by the spacecraft's 2400-Hz power bus. The voltage supplied to the short wavelength photomultiplier is fixed; that supplied to the other has two selectable values. This was done so that the gain of the multiplier structure, which varies with the voltage supplied, could be changed during the experiment to accommodate the wide range of expected light levels. The appropriate voltage is selected automatically by the limb sensors. When the light level, as determined by either of the planetary limb sensors, exceeds a predetermined level as detected by individual Schmidt trigger circuits, the high voltage to the longer wavelength sensitive photomultiplier tube is reduced to a value such that its gain is lowered by a factor of ~ 1800 . Thus spectra in the $2000\text{--}3000 \text{ \AA}$ region, that most sensitive to ozone absorption in the Hartley bands, can be recorded without saturation. The triggering of the Schmidt circuits is indicated by pulses in the shorter wavelength channel. Likewise, when the light level measured by the limb sensors falls below a second level, the high voltage to the first photomultiplier is restored to its initial value.

During the 2.82 sec when the monochromator is being scanned, a signal proportional to the photomultiplier tubes anode current, and thus proportional to the detected light intensity, is measured. The output current is integrated and amplified by a charge sensitive amplifier, and its output is then presented to an analog-to-digital converter. This converter consists

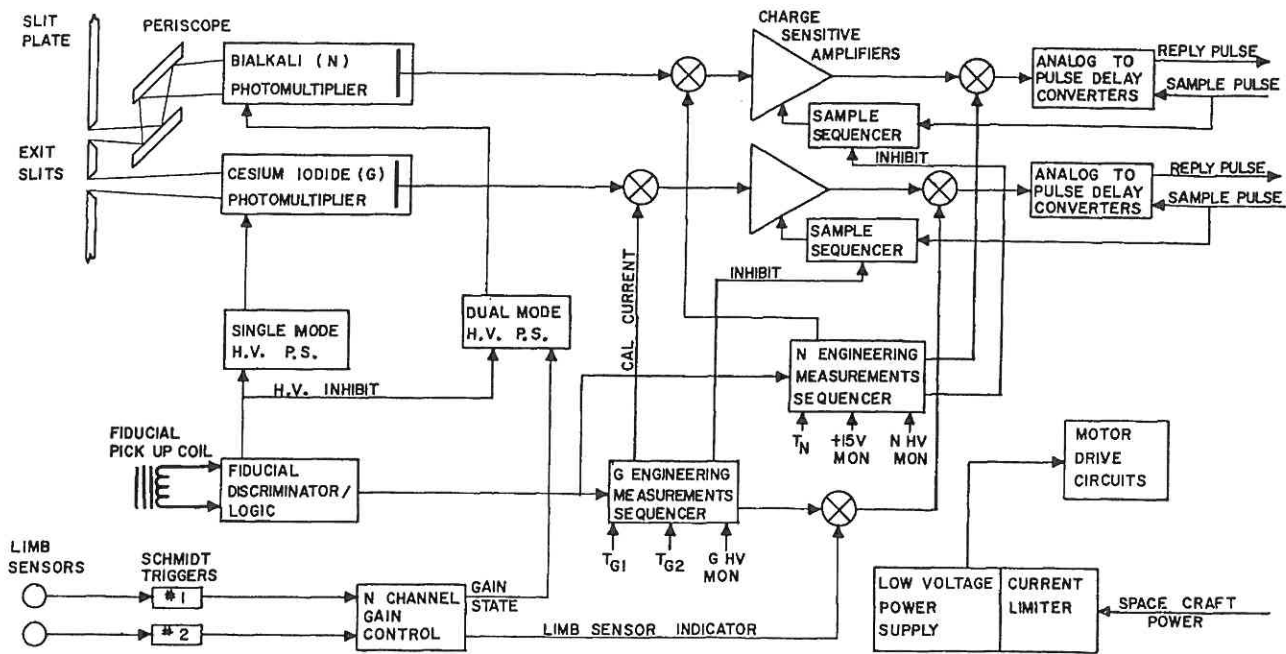


Fig. 8. Block diagram of the detector and electronics system.

of an analog-to-pulse delay converter in the instrument and a gated counter in the spacecraft data system. Figure 9 is a schematic diagram of one of the channels. Each photomultiplier tube's output is integrated and read at 5-msec intervals. The readouts occur alternately and symmetrically, thus an instrument reading is obtained each 2.5 msec. At each readout commanded by the data system, the following sequence occurs:

- (1) the voltage on the capacitor is applied to the high sample and hold amplifier (switch 1 in Fig. 9);
- (2) the photomultiplier tube input circuit integrating capacitor is shorted for 100 μ sec (switch 2);
- (3) a measure of the voltage across this capacitor is transferred to the low sample and hold amplifier (switch 3); and
- (4) the difference analog signal (high-low) is transferred to the final sample and hold circuit where it remains stored until an analog-to-digital conversion is initiated by the following read command (switch 4).

This differential method is used to negate the effect of the transients produced while shorting the integrating capacitor and the offset of the high input impedance FET emitter follower circuit used to isolate the integrating capacitor from the sample and hold amplifiers.

At a rate of one sample per channel per 5-msec interval, approximately nine samples are taken per spectral resolution element at full width. This number is independent of the diffraction order observed. Thus, every 3 sec a spectrum is produced consisting of 600 total points from each of the two detectors. Thirty-six of the samples are devoted to fiducial period measurements and 564 to spectral measurements. Since the spacecraft data automation subsystem digitizes the output of the analog-to-pulse delay converters to eight

bits, a total instrument bandwidth of 3200 bits sec^{-1} is required.

At the beginning of the 0.18-sec flyback portion of the wavelength scan, a small permanent magnet attached to the grating drive cam passes through the gap of a pickup coil fork. The resulting pulse is used as a wavelength fiducial (see Fig. 8). The following sequence is thus initiated (note: certain of the following items are referenced by capital letters in Fig. 9):

- (A) the high voltage supplied to both photomultiplier tubes is reduced to a low value;
- (B) the amplifier offset is measured while shorting its input to ground for twelve 5-msec sample periods;
- (C) a known current is injected parallel to the photomultiplier anode by means of a calibrated resistor

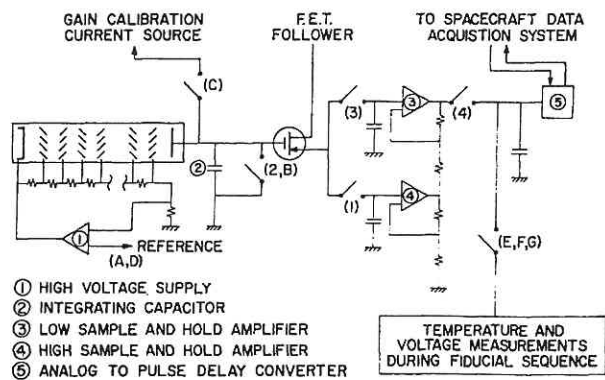


Fig. 9. Electrical schematic for a single detector channel. The letters and numbers in parentheses correspond to functional descriptions in the text.

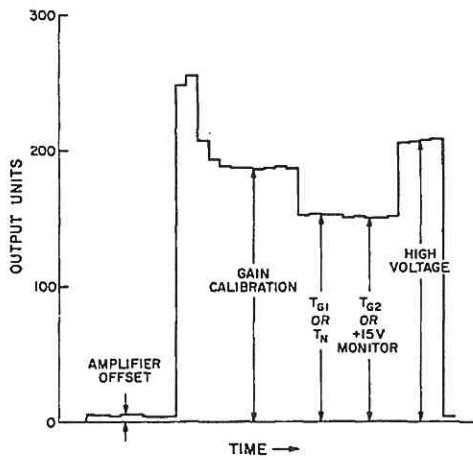


Fig. 10. The spectrometer output during a fiducial sequence.

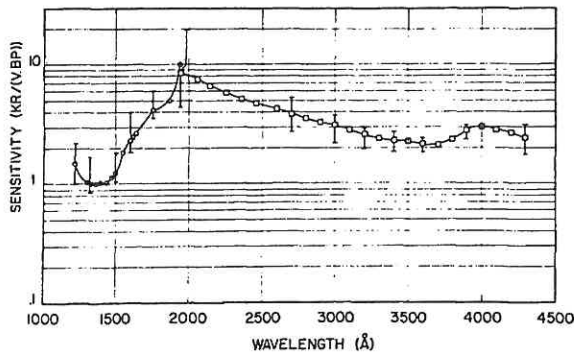


Fig. 11. The sensitivity of the Mariner 6 ultraviolet spectrometer. The points indicated by the \odot are the G channel sensitivities in kilorayleighs per volt per bandpass (nominally 10 Å). Those indicated by the \square are the N channel high gain sensitivities in kilorayleighs per volt per bandpass (nominally 20 Å).

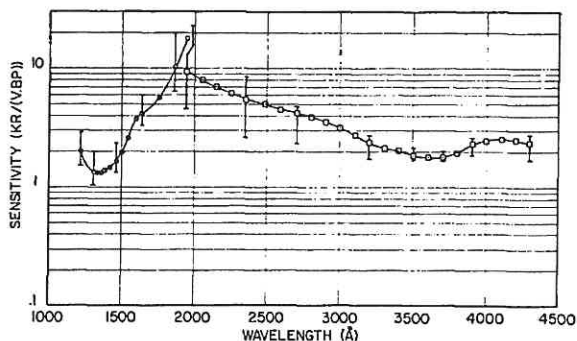


Fig. 12. The sensitivity of the Mariner 7 ultraviolet spectrometer. The points indicated by the \odot are the G channel sensitivities in kilorayleighs per volt per bandpass (nominally 10 Å). Those indicated by the \square are the N channel high gain sensitivities in kilorayleighs per volt per bandpass (nominally 20 Å).

operated from a regulated voltage for twelve samples;

(D) the high voltage is turned back on;

(E) during the turn-on transient, two temperature sensors are monitored, one by each channel, and their outputs presented the analog-to-pulse delay converters for four samples;

(F) the voltage level of the common, regulated, low voltage power supply in the case of the 1900–4300 Å (N) channel, and a second temperature in the 1100–2100 Å (G) channel is telemetered for four samples; and

(G) a voltage proportional to the now stable high voltage is presented for four samples. At this time, operation returns to the normal mode of telemetering the photomultiplier output. An example of the telemetry data during the fiducial period is given in Fig. 10.

The motor and driver circuit requires 4.1 W for operation. This combined with the 10-W requirement of the sensor electronics yields a total power consumption of 14.1 W.

Mechanical and Thermal Design

The six elements in the optical system are most sensitive to potential bending of the optical housing. Bending can cause a wavelength shift, loss of efficiency, or a total loss of signal. Sufficient thermal gradients across the case in the directions of thickness or width would cause one or more of these forms of degradation. To minimize the probability of experiencing a loss of performance under any of the anticipated environmental conditions, the instrument was machined from a single block of aluminum. This technique resulted in gradients of $\sim 2^\circ\text{C}$ under flight conditions. Gradients of this magnitude are easily accommodated by the optical system with no detectable effects on performance.

Structurally, the one-piece case proved to be rugged and reliable and had the advantage that the optical alignment was not subject to variations in torque applied to a screw, or to creep at joint interfaces during mechanical qualification and handling.

Calibration

The sensitivity in the 2800–4300 Å region was measured by recording the instrumental response to a tungsten strip lamp, of the type calibrated by the National Bureau of Standards (NBS) as a standard of spectral radiance.⁸ The instrument viewed a smoked magnesium oxide screen illuminated by the light from a 2-mm by 2-mm area of this lamp using an $f/20$ quartz lens of accurately known area. This lamp was later compared with an NBS calibrated lamp and the resultant radiance used to reduce the instrument data. Calibrations identical in technique but using different lamps and screens were performed in two different laboratories. The results were confirmed within the accuracy of the measurements. The resultant sensitivity in this range is presented in Figs. 11 and 12.

The sensitivity of the instrument was also measured at several wavelengths between 1216 Å and 2900 Å by noting its response to a collimated beam from a

monochromator illuminated with a discharge lamp. The intensity of this beam was measured using a raster scanned reference photomultiplier tube. This tube was compared to the response of a flowing nitric oxide ionization cell at 1216 Å and 1300 Å. The sensitivity of this tube at other wavelengths was determined relative to the sensitivity of sodium salicylate. This tube has been recently (April 1970) calibrated by comparison with a calibrated photodiode at NBS.⁹ A prototype instrument was calibrated in the above manner and also calibrated in the Vacuum Optical Bench (VOB) facility at the Goddard Space Flight Center. This calibration, utilizing the above and other independently calibrated reference tubes, confirmed the method used on the flight units. The sensitivity of the instruments in this region is also presented in Figs. 11 and 12.

During these calibrations the data were received by a specially constructed spacecraft data system simulator and subsequently recorded on digital magnetic tape.¹⁰ This was done so that a signal path as nearly identical as possible to that in flight could be used and to provide a library of calibration data that could be directly compared with flight data.

Instrument Performance

The Mariner 6 and 7 spacecraft, from which the observations were made, have been described.¹¹ The instrument scan platform was maneuvered in such a way that two complete limb crossing sequences were obtained on both Mariner 6 and 7 (see Fig. 3). The image of the spectrometer entrance slit was moved from high in the atmosphere down across the limb with the long dimension of the slit tangent to the limb at its center and then onto the surface for each sequence.

Figure 13 is a Mariner 7 spectrum taken when the spacecraft was 6593 km from Mars and the spectrometer was viewing the atmosphere tangentially, the optical axis being 170 km from the surface at its closest point. In addition to the emission features identified in the spectrum, there is a small amount of off-axis scattered light evident in the 2800–4300 Å region. Had the coronagraph been unable to suppress the scatter to this level, the important CO₂⁺ and atomic oxygen measurements would have been lost. The spectral resolution of the instrument is apparent from the width of the second and third order 1216-Å, hydrogen Lyman-α features. It can be seen that the transmission of several independent measurements per spectral resolution interval allows easy identification of such a feature in the presence of impulsive noise such as the feature at an apparent wavelength of 1245 Å. A measurement of the Lyman-α line, indicating the instrumental profile, is given in Fig. 14 and compared with the theoretical profile. The differences are not due to deviations in shape but rather to the statistical uncertainties in each individual measurement.

A Mariner 7 spectrum of the lower atmosphere and surface emissions is given in Fig. 15. This spectrum was taken with the N channel in the lower of its two gain states as indicated by the position of the high

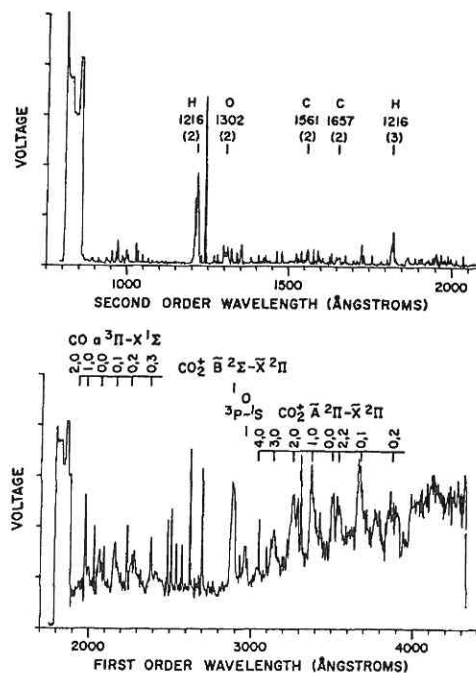


Fig. 13. The spectrum of the upper atmosphere of Mars in the 1100–4300 Å region as measured by Mariner 7. The numerals in parentheses indicate the diffraction order.

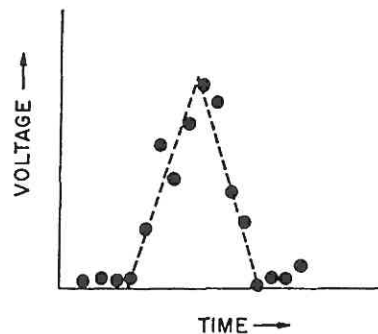


Fig. 14. An expanded view of the instrument response to an atomic line source (dots) and the theoretical profile (dashes).

voltage monitor step on the fiducial. As such, the very bright emissions are measured with a high signal-to-noise ratio. Evident are many features of the solar Fraunhofer spectrum which is diffusely reflected with an efficiency which varies slowly with wavelength. A portion of the spectrum above 3500 Å was intentionally placed off-scale so that the region from 2400 Å to 3000 Å could be emphasized. This region, unavailable to earth-based measurements, provides a particularly sensitive measure of ozone. Weak emission lines due to hydrogen and oxygen in second and third orders are seen against the much stronger scattered sunlight contribution in first and second orders in the 1800–2400 Å region in the G channel.

During the Mariner 6 and 7 encounters, 24 spectra were obtained of the upper atmosphere between 100 km and 220 km, and 475 spectra were obtained of var-

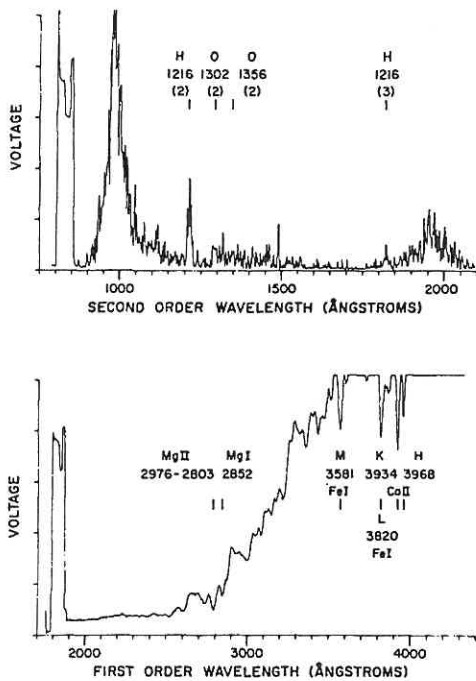


Fig. 15. The ultraviolet spectrum of Mars as measured by Mariner 7 while viewing the planet's disk. The numerals in parentheses indicate the diffraction order.

ious locations on the disk of Mars. In addition, the Lyman- α sky brightness was measured with these instruments during the weeks following the encounter.¹² During these observations, the ultraviolet spectrometers

performed flawlessly, producing spectra containing far more information than had been anticipated.

The authors wish to acknowledge the efforts of L. R. Dorman and G. McNutt for their efforts culminating in a successful experiment at Mars.

This work was supported by NASA under JPL contract 951790.

References

1. C. A. Barth, *Appl. Opt.* **8**, 1295 (1969).
2. C. A. Barth, W. G. Fastie, C. W. Hord, J. B. Pearce, K. K. Kelly, A. I. Stewart, G. E. Thomas, G. P. Anderson, and P. F. Raper, *Science* **165**, 1004 (1969); C. A. Barth, C. W. Hord, J. B. Pearce, K. K. Kelly, G. P. Anderson, and A. I. Stewart, *J. Geophys. Res.* **76**, in press (1971).
3. W. G. Fastie, *Appl. Opt.* **6**, 397 (1967).
4. H. Ebert, *Ann. Phys. Chem. n.F.* **38**, 489 (1889).
5. W. G. Fastie, *J. Opt. Soc. Amer.* **42**, 641 (1952).
6. W. G. Fastie, *J. Opt. Soc. Amer.* **42**, 647 (1952).
7. W. G. Fastie, *J. Quant. Spectrosc. Radiative Transfer* **3**, 507 (1963).
8. R. Stair, R. G. Johnston, and E. W. Halbach, *J. Res. Nat. Bur. Stand.* **64A**, 291 (1960).
9. R. Madden, photodiode calibrated at NBS, Washington, D. C.
10. R. E. McCullough, papers and presentations of Digital Equipment Computer Users' Society, Fall (1969).
11. C. E. Kohlhase, H. W. Norris, J. A. Stalkamp, and H. M. Schurmeier, *Astronaut. Aeronaut.* **7**, 80 (1969).
12. C. A. Barth, *Astrophys. J. Lett.* **161**, L181 (1970).

Annual Conference on Holography and Optical Filtering Huntsville, Alabama 24-25 May 1971

The theme of this conference, to be held at the Marshall Space Flight Center, is advancements in holography and optical filtering. Sponsored by the National Aeronautics & Space Administration and the Huntsville Section of the Optical Society of America, the conference will review research in the above areas being conducted by various NASA centers as well as numerous top professionals in industry and universities. The meeting will last for two days without parallel sessions. A program, including abstracts, will be available prior to the conference and a Proceedings will be published. For further information contact John R. Williams, Conference Chairman, NASA/MSFC, S&E-SSL-PO, Huntsville, Alabama 35812.